Received: 6 July 2020 | Revised: 16 November 2020 | Accepted: 27 November 2020
DOI: 10.1002/pen.25614

RESEARCH ARTICLE

POLYMER ENGINEERING AND SCIENCE

Evaluation of healing models to predict the weld line strength of the amorphous thermoplastic polystyrene by injection molding simulation

Jakob Onken | Steffen Verwaayen | Christian Hopmann

Institute of Plastics Processing, RWTH Aachen University, Aachen, Germany

Correspondence
Steffen Verwaayen, Institute of Plastics Processing, RWTH Aachen University, Seffenter Weg 201, 52074 Aachen, Germany.
Email: steffen.verwaayen@ikv.rwth-aachen.de, sekretariat@ikv.rwth-aachen.de

Funding information
German Bundesministerium für Wirtschaft und Energie (BMWi), Grant/Award Number: 18132N

Abstract

In many injection molded parts weld lines are often unavoidable. These cause optical defects and a reduction of the mechanical properties of the part. Therefore, the predictability of the weld line strength at an early stage of development would provide a significant advantage by avoiding costly iterations of the mold and increases the understanding of the correlation between process history of the melt and weld line strength. For this purpose, a calculation routine has been developed to predict the weld line strength based on injection molding simulation. Different models to calculate the healing of a weld line are compared and analyzed. By adding a factor to consider the shear rate in addition to the temperature and the pressure and after calibration to one design of experiment setting of the experimental data, the prediction of the weld line strength shows good agreement for all examined process setpoints of the experimental data for polystyrene.

KEYWORDS

amorphous thermoplastics, injection molding, modeling, simulations

1 | INTRODUCTION

Weld lines can reduce the static strength of the part by up to 50%. The extent of this reduction in strength is highly dependent on the material used. In addition, weld lines often cause optical defects.[1, 2] A weld line is formed when two or more melt fronts meet in the cavity during the injection molding process. Most commonly this is caused by flow obstacles, which divide the melt front. Other reasons can be multiple flow fronts due to multiple gates or different local melt acceleration as a result of different flow resistances based on different wall thicknesses.[3] While weld lines should be avoided by a proper part and mold design, this is usually not possible. Especially if weld lines result from flow obstacles. Moving the weld line to a less stressed area of the part by moving the gate is also only possible to a limited extent.[4, 5] The uncertainty regarding the mechanical properties in the weld line leads to problems. One such problem is the oversizing of parts to account for the uncertain weld line strength. Another problem can be overall part failure due to the weld line failing before bulk material failure. Both cases are detrimental to economic efficiency. Therefore, the prediction of the weld line strength already at the design stage is essential to prevent oversizing or premature part failure.[4–6]

In the characterization of weld lines, a distinction is made between stagnating and flowing weld lines (Figure 1). Stagnating weld lines are formed during frontal contact and subsequent stagnation of the flow front in the

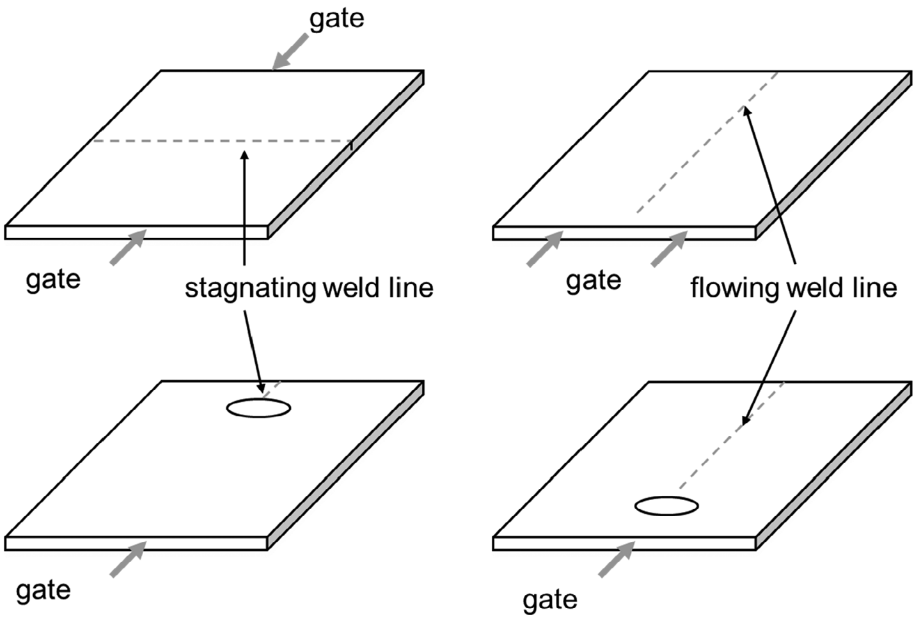

FIGURE 1 Formation of stagnating (left) and flowing weld lines (right) using the example of an injection-molded plate with circular flow obstacle and different gate positions

weld line. Flowing weld lines are created when the flow fronts meet at a sharp angle and then continue to flow.[4]

The decrease of the strength of weld lines can be explained by the lack of interdiffusion of the molecular chains across the interface, the strong molecular orientation in the weld line due to higher shear rates and the stress concentration through a V-shaped notch at the plate surface along the weld line.[3, 4, 6–11]

When the melt fronts meet, the molecular chains of the separate melt fronts are not entangled beyond the interface. Gradually, the molecular chains diffuse beyond the interface of the weld line and begin to entangle. If the chain entanglement is the same as before the melt separation, the original material strength is restored. High temperatures and a long diffusion time are particularly beneficial for interdiffusion. The temperature has to exceed the glass transition temperature for amorphous thermoplastics or the crystallite melting temperature for semi-crystalline thermoplastics.[4, 9] This contradicts the target of short cycle time in the injection molding process for cost-effective production.

Strong molecular orientation results from the expansion flow of plastic melts. The molecules located in the flow front are oriented orthogonal to the flow direction. In stagnant weld lines in particular this orientation is frozen in transverse direction to the direction of flow.[9, 12] In addition, interdiffusion at the interface is reduced by a shear-induced deformation of the molecular clusters.[13] Furthermore, the formation of a so-called V-notch can reduce the mechanical strength. This is due to a stress concentration in the weld line under load.[11, 14, 15] The origin of V-notches is not yet fully understood. Explanation approaches are the relaxation of the strongly oriented molecules or air inclusions in the weld line.[1, 16–19]

2 | HEALING OF WELD LINES

In general, a complete healing, that is, a recovery of the weld line to the original mechanical properties of the material is possible. However, in reality there is usually only partial healing mainly due to interdiffusion processes in the interface, which are influenced by the process, the part geometry, and the material.[20] The greater the difference between melt temperature and glass transition temperature, the faster the interdiffusion. Below the glass transition temperature, the interdiffusion is negligible.[21, 22] An increase in holding pressure should also result in a positive effect.[23, 24] The holding pressure time, cooling time, and mold temperature only show a small influence on the weld line strength.[5, 24, 25]

Often, the weld line factor F_{WL} is used to describe the weld line strength. It is defined as the ratio of the strength of the weld line σ_b to the strength of the undisturbed material σ_u without weld line[5, 26]:

$$F_{WL} = \frac{\sigma_b}{\sigma_u}. \tag{1}$$

Since it is often impossible to avoid weld lines as well as a limited possibility to increase the weld line strength by adjusting the injection molding parameters, a method to predict the weld line strength in the product development process is shown below.

2.1 | Prediction of weld lines with injection molding simulation software

The simulation of the injection molding process enables the description and prediction of the manufacturing process of injection molded parts. This allows for the investigation of the thermal and rheological conditions during the filling process. Commercially available programs for injection molding simulation allow the prediction of the position of weld lines.[23] However, a quantitative prediction of the weld line strength is impossible yet.

There are various investigations that consider the simulated thermo-rheological state in the weld line in order to correlate it to the weld line strength. Correlations of the viscosity or temperature profile in the weld line with the weld line strength were found.[18, 27, 28] However, these only allow a qualitative prediction of the weld line strength, which can only be used to a very limited extent as a basis for part design.

Therefore, the suitability of different models for describing the healing of weld lines is investigated below. The aim of the investigated models is the quantitative prediction of weld line strength based on injection molding simulation. The required calibration of the models is carried out at different design of experiment (DoE) settings to show the influence of the calibration. To compare the different models, the respective results of the weld line strength prediction are shown. In addition, the factors taken into account for the weld line strength prediction of the different models are compared.

2.2 | Design of experiment

The investigations of weld lines are carried out on injection-molded plates of 114 mm x 125 mm size and 2 mm thickness made of polystyrene as shown in Figure 2. Two flow barrier geometries are used for the investigation. First, a circular flow barrier with a diameter of 20 mm. And second, a rectangular flow barrier with a width of 40 mm and a height of 20 mm. In addition to the plates shown in Figure 2, plates without flow obstacle and thus without weld line are produced for reference tests. During production, the melt temperature and the pressure are varied in three steps (+, 0 and −). Test specimens are taken from the plates at distances of 5, 25, and 45 mm from the flow obstacle (Figure 2, left). The mechanical test results used for this work were already published, so they will be not discussed here again.[29, 30]

For the evaluation of the mathematical models to predict the weld line strength the results of the tensile tests for polystyrene behind the rectangular flow obstacle are used.

2.3 | Simulation model to predict the formation of the weld line

For the simulations presented in this paper, the injection molding process simulation software SigmaSoft, version

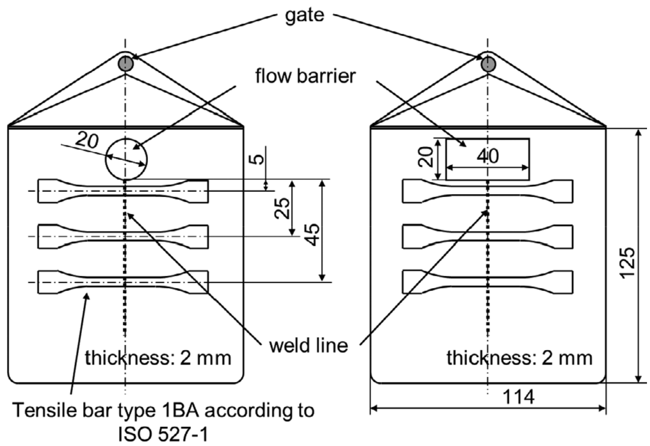

FIGURE 2 Injection-molded PS and PMMA plates for the generation of test specimens with weld lines and position of the test specimens. PMMA, polymethyl methacrylate

5.2.1.0 of SIGMA Engineering GmbH, Aachen, Germany, is used. The material data required for the simulations were specifically measured and determined for these investigations. The software used is based on the finite volume method. The part is meshed using hexahedral elements. For a good resolution of the rheological and thermal conditions inside the cavity, a mesh with seven elements over the thickness of the part is created. The temperatures, pressures, and shear rates determined in the simulation are exported and used as the basis for the healing models described below.

2.4 | Reptation model by de Gennes

One approach used for modeling the healing of a weld line is the reptation model by de Gennes.[31] Originally the model describes the molecular movement of individual polymer chains interacting with their environment. In the process of interdiffusion in a weld line the polymer chains have to move across the weld line interface in order to restore the entanglements of the polymer and thus regain the original material strength. Therefore, the mathematical description of the reptation time is used to describe the weld line strength.

The reptation model is based on the assumption that a polymer chain can move freely within a tube but can only leave the tube via its ends (Figure 3). Any other movement beyond the tube is prevented by entanglement with the surrounding molecules.

The thermal energy of the melt enables the movement of the polymer chains. Thus, higher temperatures lead to a higher mobility of the polymer chains, which reduces the so-called reptation time t_{rep}.[31] With the help of the reptation model the reptation time can be determined. The reptation time defines the average time a

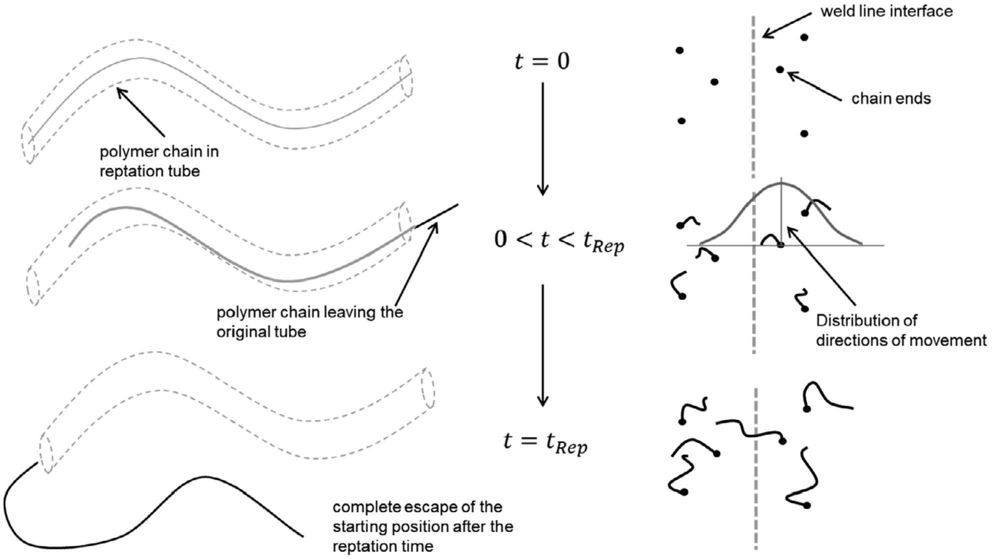

FIGURE 3 The reptation theory and its influence on the healing of weld lines[31, 32]

polymer chain needs to completely escape the initial tube (Figure 2, left). It is significantly influenced by the temperature of the melt and its rheological properties. An approach for the calculation of the reptation time was developed by Kim and Wool.[33, 34] The temperature dependent reptation time t_{rep} can be calculated using the entanglement molar mass M_e, the density ρ, the zero viscosity η_o, the ideal gas constant R, and the temperature T of the polymer (Equation (2)).

$$t_{rep}(T) = \frac{20M_e}{\pi^2 RT\rho}\eta_0. \tag{2}$$

Reptation of the polymer chains also takes place across weld lines and thus contributes significantly to the healing of weld lines.[22, 33] This is shown schematically on the right of Figure 3. Experimental studies showed that the weld line factor σ_b/σ_u is proportional to the fourth root of time available for a weld line to heal in the molten isothermal state[22, 33]:

$$\frac{\sigma_b}{\sigma_u} \propto t^{0.25}. \tag{3}$$

Kausch and Tirrell introduced the following relationship in order to determine the weld line strength as a function of the reptation time under isothermal conditions:

$$\frac{\sigma_b}{\sigma_u} = \left(\frac{t}{t_{rep}}\right)^{0.25}. \tag{4}$$

The reptation model has already been validated by various molecular dynamic and experimental studies.[35–38]

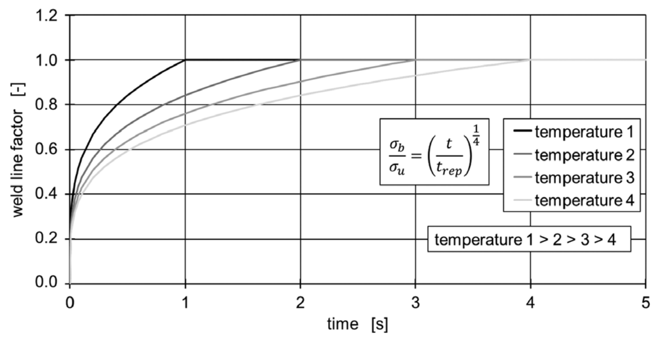

FIGURE 4 Exemplary healing progression of a weld line interface according to the reptation model at different temperatures

If the model is applied to the movement of polymer chains across weld lines and thus to their healing, the mathematical formulation results in a healing process in the form of a root function, as exemplary shown in Figure 4. A higher cooling rate results into slower healing. To prevent physically reasonable values greater than 1, the healing must be terminated at this value.

2.5 | Influencing factors on the reptation time

The reptation time is calculated using the entanglement molar mass M_e, the density ρ, the zero viscosity η_o, the ideal gas constant R, and the temperature T. Thus, there is a direct dependence on the temperature. For the description of the zero viscosity the Carreau-WLF-model is used[39]:

$$\eta(T,\dot{\gamma}) = \frac{\eta_0}{(1+B\dot{\gamma}a_T)^C} \text{ with } \eta_0 = A\cdot a_T. \tag{5}$$

Here η is the shear rate- and temperature-dependent viscosity, η_o the zero viscosity, A, B, and C are model parameters, and a_T the temperature shift parameter of the Williams-Landel-Ferry (WLF) equation.

In addition to the influence of temperature, an influence of the pressure in the part on the weld line strength is observed in our previously published studies.[29] In these experimental studies, an increase in holding pressure leads to a reduction in weld line strength, which is in contrast to what literature states for amorphous thermoplastics. One reason for this could be the high pressure dependence of viscosity of polystyrene. Under higher pressure the viscosity rises and thus inhibits the interdiffusion. To illustrate this influence in the model, an extension of the WLF equation according to Menges, Wortberg, and Michaeli[39–41] is used. The calculation of the shift factor a_T includes, in addition to the shift in viscosity due to temperature, a shift due to local pressure (Equation (6)). Here T_0 represents the reference temperature, T_S the standard temperature, and T the local temperature. The parameter f_p is the pressure shift factor. This can be approximated by the displacement of the glass transition temperature with the pressure determined from pvT data.[42]

$$a_T = e^{\left(\frac{8.86(T_0 - T_S)}{101.6^\circ C + T_0 - T_S} - \frac{8.86(T - T_S - f_p \cdot p)}{101.6^\circ C + T - T_S - f_p \cdot p}\right)}. \tag{6}$$

This formulation of the temperature and pressure dependence of viscosity means that the calculated zero viscosity decreases with increasing temperature and increases with increasing pressure. Used in Equation (2), increasing temperature decreases the reptation time and thus the healing of the interface is faster, while an increase in pressure provides a higher reptation time and thus slower healing. This is also consistent with the assumption that a higher pressure gives a reduction of the free volume in the plastic melt and thus to poorer healing of the weld line.

The density is described using the modified 2-domain Tait model.[43] The model describes the specific volume ν, which is the reciprocal of the density ρ, as a function of pressure and temperature.

The entanglement molar mass M_e is the statistical average molecular weight of the part of one polymer chain, which lies between two entanglements of this chain with other polymer chains from its surroundings. M_e thereby describes in an implicit way the degree of entanglement of the polymer chains among themselves. In this research, the literature values for polystyrene are used.[44]

In previously published studies, the weld line strength could be correlated with the local shear rate.[30] This is not taken into account in the model presented so far, which is based on the reptation model. A consideration of the shear rate would be possible by replacing the zero viscosity in Equation (2) by a simulated dynamic viscosity. However, a higher viscosity is also found in those areas where greater healing is observed. Thus, an increase of the dynamic viscosity would lead to a higher reptation time and thus to slower healing in areas with actually high weld line factors. Therefore, this exchange is not useful.

In addition to the experimental investigations in this work, investigations by Yokomizo et al.[13] indicate that shear deformation of the melt inhibits reptation. Therefore, the described model is extended by a factor β to integrate the observed influence of the shear rate into the model to improve the prediction of the weld line strength. For the integration of the shear rate into the reptation model, the reptation time needs to be multiplied by a factor depending on the shear rate.[32] The factor should not change the reptation time at a shear rate of zero but increase the reptation time with increasing shear rates. The investigations show a nonlinear relationship between shear rate and weld line factor, which can be represented by a logarithmic function:

$$\beta_{rep}(\dot{\gamma}) = 1 + \ln\left(b_{rep}\dot{\gamma} + 1\right). \tag{7}$$

Here β_{rep} represents a shear rate-dependent function, b_{rep} a calibration factor, and $\dot{\gamma}$ the shear rate. The logarithmic function does not change the reptation time at a shear rate of 0 1/s but increases the reptation time exponentially with increasing shear rate. The factor b_{rep} defines the slope and must be calibrated based on experimental results.

The consideration shown above results in a temperature-, pressure-, and shear rate-dependent description of the reptation time as shown in Equation (8). In addition, the constant $1/C_{rep}$ is added, which is calibrated by experimental results.

$$t_{rep}(T,p,\dot{\gamma}) = \beta_{rep}(\dot{\gamma}) \frac{20M_e}{\pi^2 R T \rho(T,p)} \eta_0(T,p) \frac{1}{C_{rep}}. \tag{8}$$

2.6 | Time discretization for the reptation model

The formulation of the reptation time is based on isothermal and isobaric conditions. However, in the injection molding process anisothermal and anisobaric conditions are present. Anisothermal formulations of the reptation model utilizing a time discretization are found in the investigations of Bastien and Gillespie.[45] In addition to the anisothermal and anisobaric calculation of healing, this also allows the use of results of injection molding simulations, as these are only available in a time-discrete form.

The formulation of the incremental healing in Equation (9) showed the best agreement with experimental results in the studies of Bastien and Gillespie.[45] In the equation dH_i represents the healing increment at time i. The healing increment is calculated in the same way as in Equation (4) from the elapsed time at time i and $i+1$ and the reptation time of the respective time i.

$$dH_i = \frac{{t_{i+1}}^{0.25} - {t_i}^{0.25}}{{t_{rep,i}}^{0.25}}. \tag{9}$$

The total healing, and respectively, the weld line factor is determined by summing up the individual healing increments (Equation (10)).

$$\frac{\sigma_b}{\sigma_u} = dH = \sum dH_i. \tag{10}$$

The termination criterion for calculating the healing increments is reaching a weld line factor of 1 or falling below the pressure-dependent glass transition temperature T_G.

2.7 | Interdiffusion model according to Kim and Suh

Another approach to calculate the weld line strength is the interdiffusion model of Kim and Suh,[6] which describes the healing of polymer-polymer interfaces based on molecular interdiffusion. With the approach of Kim and Suh, the weld line factor can be represented as a function of the ratio of two surfaces (Equation (11)). A_0 represents the total interface in the weld line. A is the area where interdiffusion has not yet taken place (Figure 5).

$$\frac{\sigma_b}{\sigma_u} = 1 - \frac{A}{A_0}. \tag{11}$$

The change of the area A where no interdiffusion has taken place over time is determined by a diffusion equation (Equation (12)). D represents the interdiffusion coefficient, ΔG the change in free enthalpy, k the Boltzmann

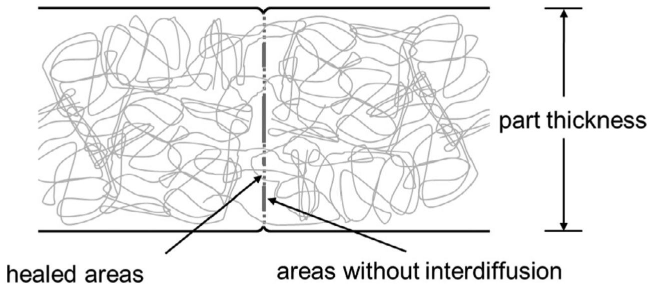

FIGURE 5 Healing of a weld line according to the model of Kim and Suh[6, 32]

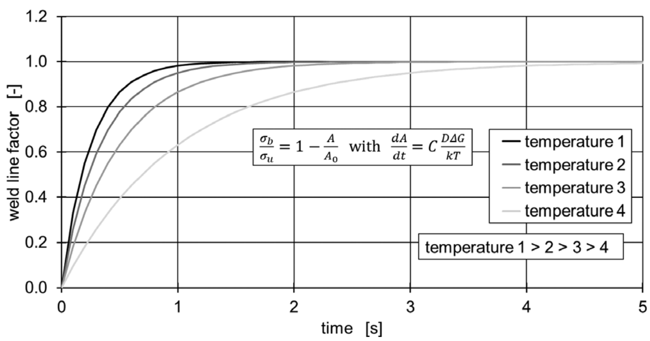

FIGURE 6 Exemplary healing process of a weld line interface according to the interdiffusion model at different temperatures

constant, and C_{diff} a constant, which can be used to calibrate the model.[6]

$$\frac{dA}{dt} = C_{diff}\frac{D\Delta G}{kT}. \tag{12}$$

Mathematically the healing curve of the interdiffusion model follows an exponential function, which asymptotically approaches the value 1. In contrast to the reptation model there is no need to terminate the healing. The healing curve is exemplary illustrated in Figure 6.

The free enthalpy ΔG is composed of the surface tension of the melt γ, the area A, the temperature T, and the mixture entropy ΔS (Equation (13)).

$$\Delta G = -2\gamma A - T\Delta S. \tag{13}$$

Since the mixture entropy of high polymer materials is negligible, in the following only the surface tension is considered.[22, 46] Inserting Equation (13) with $\Delta S = 0$ in Equation (12) results in Equation (14). If this equation is solved for A, subsequently integrated and then inserted into Equation (11), the weld line healing or the weld line factor can be calculated according to Equation (15).

$$\frac{dA}{dt} = -\frac{D2\gamma A}{kT} C_{diff}, \quad (14)$$

$$\frac{\sigma_b}{\sigma_u} = 1 - e^{-\frac{D2\gamma t}{kT} C_{diff}}. \quad (15)$$

For the calculation of the interdiffusion coefficient D there are different approaches, which are generally based on rheological and thermal material data.[21, 47] Two such approaches will be used in the scope of this work and will be presented in the following.

The first approach to determine the diffusion coefficient is the approach provided by Bueche (Equation (16)).[48] The diffusion coefficient is dependent on the mean square end to end distance R_e^2 and the mean molecular weight M_W of the polymer as well as the density ρ, the Avogadro constant A_G, the Boltzmann constant k, the temperature T, and the dynamic viscosity η of the plastic melt. The diffusion coefficient of a given material is thus dependent on density, temperature, and viscosity, since the other values are material constants.

$$D_B(\rho, T, \eta) = \frac{\left(\frac{A_G \rho k T}{36}\right)\left(\frac{R_e^2}{M_w}\right)}{\eta}. \quad (16)$$

The second approach used is the diffusion coefficient of the model according to Doi and Edwards (Equation (17)).[21] Here, the diffusion coefficient is a function of the plateau module G_0, the density ρ, the ideal gas constant R, the mean square end to end distance R_e^2, the mean molecular weight M_W, and the critical molecular weight M_C, which describes the minimum molar mass of a polymer chain needed for forming entanglements, and the zero viscosity η_0. As such, this model determines the diffusion coefficient, apart from material constants, only as a function of density, temperature, and zero viscosity.

$$D_{DE}(\rho, T, \eta_0) = \frac{G_0}{135}\left(\frac{\rho R T}{G_0}\right)^2 \left(\frac{R_e^2}{M_w}\right) \frac{M_C}{M_w^2 \eta_0}. \quad (17)$$

2.8 | Influencing factors on the interdiffusion

The temperature directly influences both the interdiffusion and the two presented interdiffusion coefficients. Furthermore, the density present in both interdiffusion coefficients is influenced by temperature and pressure. The zero viscosity of the interdiffusion coefficient D_{DE} also is dependent on temperature and pressure. For the calculation of the interdiffusion coefficient D_B, the local dynamic temperature- and shear rate-dependent viscosity calculated by the injection molding simulation is used.

Just like the reptation model, the interdiffusion model does not take the shear rate into account for modeling the healing of the weld line. Therefore, similar to the reptation model, a factor is integrated, which reduces the healing rate with increasing shear rate. To achieve this, the interdiffusion coefficient is multiplied by a factor, which decreases with increasing shear rate and thus reduces the calculated healing.[32]

The factor must not change the interdiffusion coefficient at a shear rate of zero. For the description of the nonlinear relationship, the use of an exponential function is obvious (Equation (18)). In the equation b is a factor that has to be calibrated for the material used with experimentally determined values and $\dot{\gamma}$ is the shear rate. The exponential function allows the factor β to have a value of 1 at a shear rate of 0.1/s. Thus, the diffusion coefficient is not affected at this shear rate. As the shear rate increases, the function asymptotically approaches a value of 0. Thus, when the diffusion coefficient is multiplied by β, the interdiffusion is increasingly inhibited with increasing shear rate.

$$\beta_{diff}(\dot{\gamma}) = e^{-b_{diff}\dot{\gamma}}. \quad (18)$$

Integration of these factors in Equation (15) results in the temperature, pressure, and shear-rate dependent description of weld line healing as presented in Equation (19).

$$\frac{\sigma_b}{\sigma_u}(T, p, \dot{\gamma}) = 1 - e^{-\frac{D(T,p)\beta_{diff}(\dot{\gamma})2\gamma t}{kT} C_{diff}}. \quad (19)$$

2.9 | Time discretization for the interdiffusion model

The healing process of the interdiffusion model follows an exponential function. Thus, the function follows a steep gradient at the beginning and subsequently asymptotically approaches a value 1. For each healing increment dH_i the previous theoretical healing at the given process conditions at time i must be subtracted (Equation (20)). If this is not done, the maximum healing of 1 may be exceeded, which would represent an unphysical value.

$$dH_i = \left(1 - e^{-\frac{D\beta_{diff} 2\gamma t_{i+1}}{kT_i} C_{diff}}\right) - \left(1 - e^{-\frac{D\beta_{diff} 2\gamma t_i}{kT_i} C_{diff}}\right). \quad (20)$$

Furthermore, a sensitivity analysis in previous investigations shows that the summation of the individual increments may results in calculated weld line factors of more than 1, which is physically unreasonable. Therefore, the healing increments are normalized to the remaining possible healing in each time step. The sum of the normalized healing increments results in the total healing of the weld line factor (Equation (21))

$$\frac{\sigma_b}{\sigma_u} = dH = \sum dH_{i,T_i} \frac{1 - dH_{i-1,T_{i-1}}}{1 - dH_{i-1,T_i}}. \tag{21}$$

3 | MECHANICAL MODELING

For a structural-mechanical simulation of injection molded parts made of amorphous unfilled thermoplastics with weld lines, the weld lines must also be modeled mechanically. The most important aspect of this is the way in which the weld line factor calculated with the models presented is integrated into the structural simulation.

There are a few requirements for the mechanical modeling. The macromechanical behavior of the parts must not be influenced by the weld line. The shear strength of the weld line must be higher than the tensile strength of the material without weld line. The crack initiation occurs in the outer layers of the weld line and the failure of the weld line is abruptly without previous damage.

Since the macromechanical behavior of the parts is not influenced by the weld line, an elastoplastic description of the stress–strain behavior can be used for the parts.[49]

Previously published studies have shown that the shear strength of the weld lines is higher than the tensile strength of the undisturbed material.[29] Therefore, the normal stress hypothesis is used to determine the stresses present in the part. Thus, the part fails if the normal stress exceeds the breaking stress.

To take into account the sudden failure of the weld line without prior damage, the calculated weld line factor is implemented as a local reduction factor of the breaking stress. Consequently, the part fails as soon as the breaking stress of the weld line is exceeded.

The structure of the integrative calculation routine was already published in References [30, 50], and is therefore, not explained here.

To use the calculation routine, the investigated models must first be calibrated once for the material used. Then the different models are compared. The calibration of the models is carried out using the calibration factors C and b (Equations (7), (8), (12), and (18)). The calibration of the various models is based on tensile tests and injection molding simulations presented in.[29, 30] For calibration, the injection molding process of the plates and the experimental testing of the tensile bars is simulated. In addition to the results of the modeling, the influence of the process condition, that is, DoE settings selected for calibration on the calculated weld line factors is also compared. For this purpose, the calibration is exemplary carried out at the DoE settings (++), (00), and (−−).

Figure 7 shows an example of the predicted weld line factors used in a structural simulation in the software Abaqus of DS Simulia, Providence, RI, USA. The test bar is taken from a plate made of polystyrene at a distance of 5 mm behind a rectangular flow obstacle. The weld line factors shown are calculated by the reptation model. It can be seen that the simulation predicts a low weld line factor in the surface layers of the part. In the middle of the part the original strength of the material is restored. The weld line strength also decreases with increasing distance from the flow obstacle, which is in agreement with the experimental results.

3.1 | Calibration and evaluation of the presented models to predict the weld line strength

In the following, the results of predicting the weld line factors using the three modified models introduced above are presented for different process parameters. In addition, the influence of the calibration at different DoE settings is compared to show the influence of the calibration and to find the best setting to calibrate the routine. In previous experimental investigations, plates made of polystyrene with rectangular flow barrier show the clearest dependence of weld line strength on process and flow barrier geometry. Therefore, they are used as examples for the comparison of the models and the calibration procedure.[32]

3.2 | Evaluation of the interdiffusion model with the diffusion coefficient D_{DE} and of the calibration at different DoE settings

Figure 8 shows the experimentally determined weld line factors compared to the weld line factors calculated by the interdiffusion model with the diffusion coefficient D_{DE} according to Doi and Edwards (Equation (17)).[21] Furthermore, model calibration at different DoE settings and distance to the flow obstacle is shown. The DoE settings shown are (++), (00), and (−−). The DoE setting for which the weld line factors were measured and predicted is shown above the graph. The experimentally determined weld line factors as a function of the distance to the flow obstacle are shown on the left-hand side (Exp.) on each paragraph. On the right-hand side, the weld line factors as a function of the distance to the flow obstacle as calculated by the weld line routine are shown. The DoE setting used for calibration of the routine is given below the respective graph. For example, the bars on the far right of the left graph show the weld line factors for the DoE setting (++) as indicated above the graph calculated with the weld line routine, which was

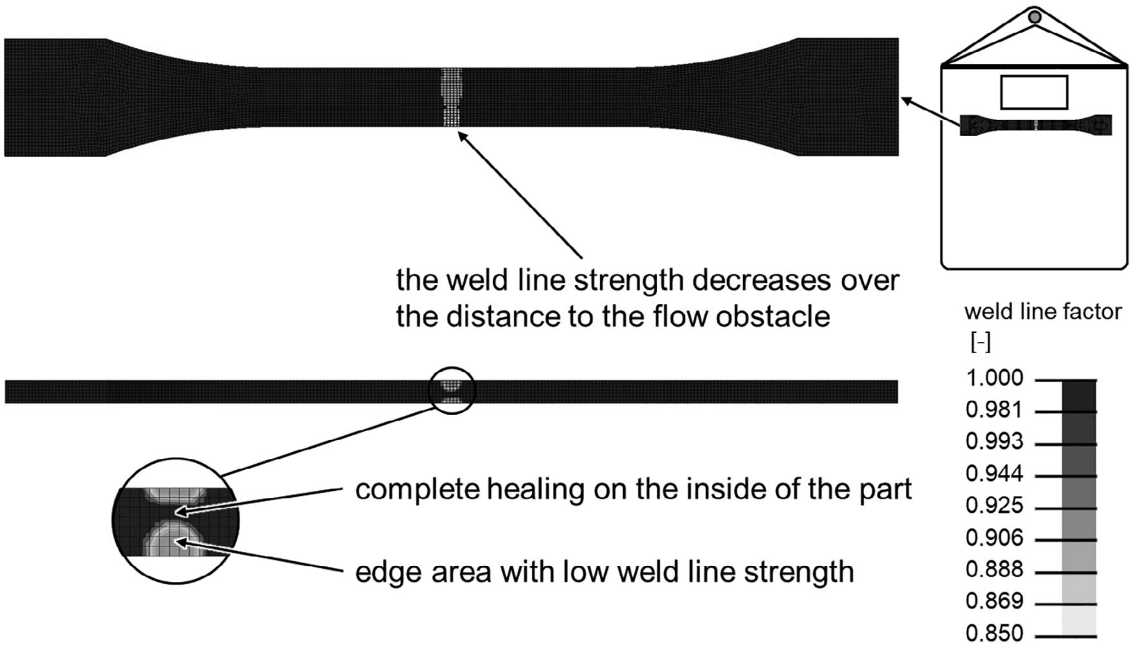

FIGURE 7 Weld line factors calculated using the reptation model for a tensile bar made of PS at a distance of 5 mm from the flow obstacle of a plate with a rectangular flow obstacle at DoE setting (00)

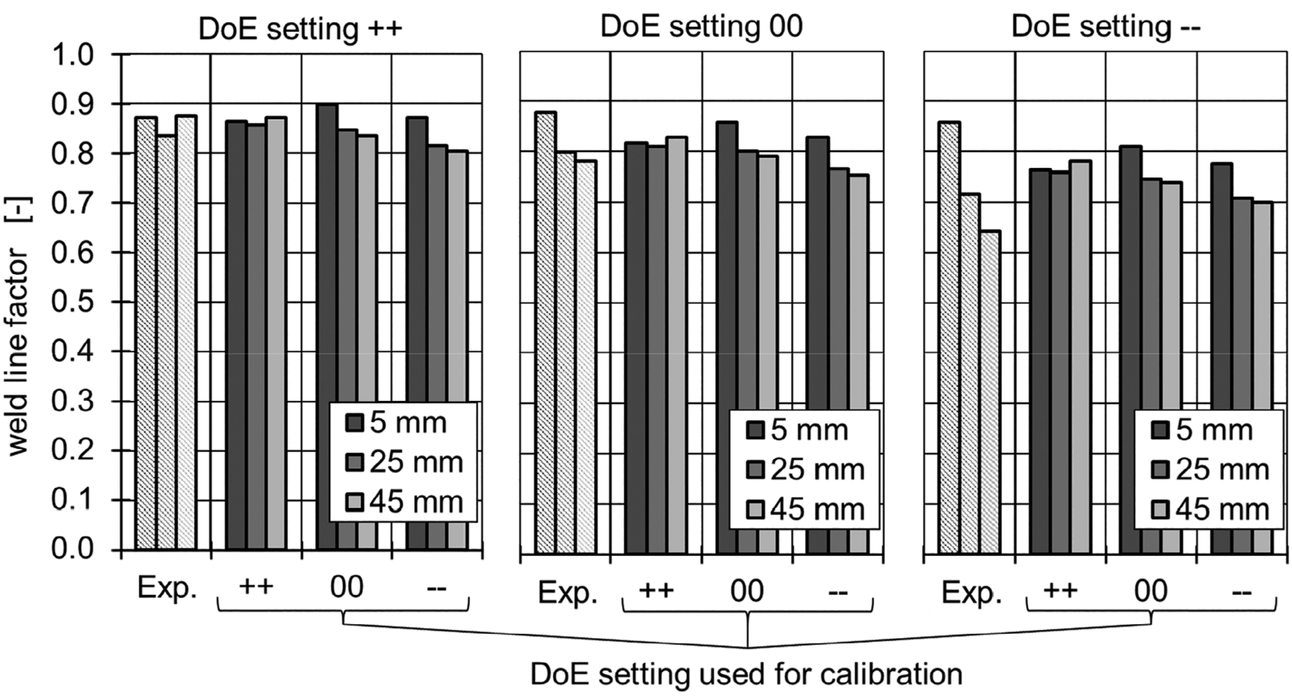

FIGURE 8 Weld line factors for polystyrene plates with rectangular flow barrier calculated using the interdiffusion model with D_{DE}

previously calibrated at the DoE setting (−−) as indicated below the graph.

The best agreement between the weld line factors determined experimentally and the weld line factors determined by simulation is found if the weld line routine is calibrated at the corresponding DoE setting (second column in the first graph, third column in the second graph, and fourth column in the third graph). Both the quantitative values as well as the qualitative progressions are best met. Only at the DoE setting (−−) higher deviations can be found. Since calibration at the DoE setting, which should be predicted is not useful, one DoE setting for calibration to predict all other DoE settings should be used. The best DoE setting for calibration to predict all DoE settings is DoE setting (00), thus the central point. Here, the deviations in the prediction are the smallest on average with an error value of 0.0545. However, the qualitative progression over the distance to the flow obstacle cannot be represented correctly for DoE setting (++).

3.3 | Evaluation of the interdiffusion model with the diffusion coefficient D_B and of the calibration at different DoE settings

In Figure 9 the weld line factors are determined by the interdiffusion model with the diffusion coefficient D_B (Equation (16))[48] analogous to Figure 8.

When using the diffusion coefficient according to Bueche, as with the diffusion coefficient D_{DE}, the greatest agreement is achieved if the corresponding DoE setting is used for calibration. Likewise, the best average prediction results for all DoE settings is achieved by calibration at the central DoE setting (00) with an error value of 0.0943. However, the qualitative course of the prediction in particular is represented with lower accuracy when compared to using the diffusion coefficient D_{DE}. This is mainly due to the fact that in the model according to Bueche, the dynamic viscosity is included in the description of the diffusion coefficient. Here, a higher shear rate causes the dynamic viscosity to decrease. This increases the diffusion coefficient and thus the weld line healing (Equation (16)). This contradicts the observations that an increased shear rate slows down interdiffusion. The influence of the introduced factor β_{diff} (Equation (18)) is thus reduced by the use of dynamic viscosity in the diffusion coefficient.

3.4 | Evaluation of the reptation model and of the calibration at different DoE settings

In Figure 10, the weld line factors are determined using the reptation model[31] analog to Figure 8.

As with the interdiffusion model, the best agreement between the weld line factor determined experimentally

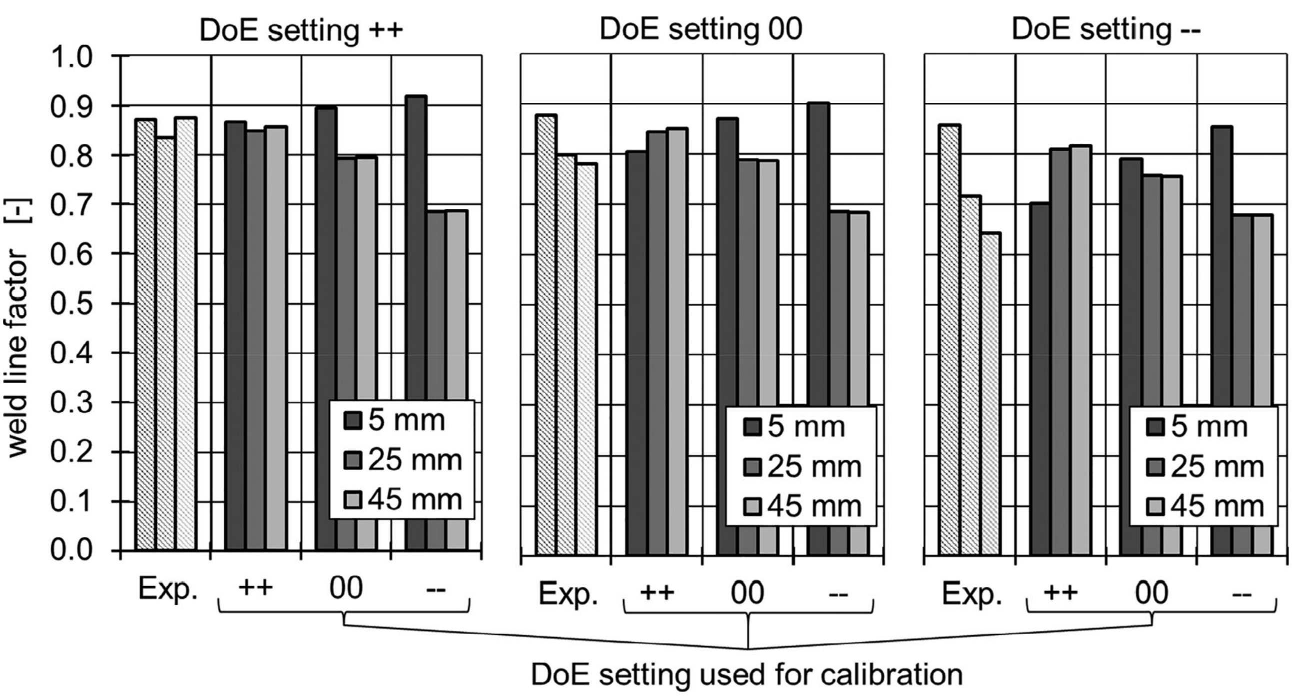

FIGURE 9 Weld line factors for polystyrene plates with rectangular flow barrier calculated using the interdiffusion model with D_B

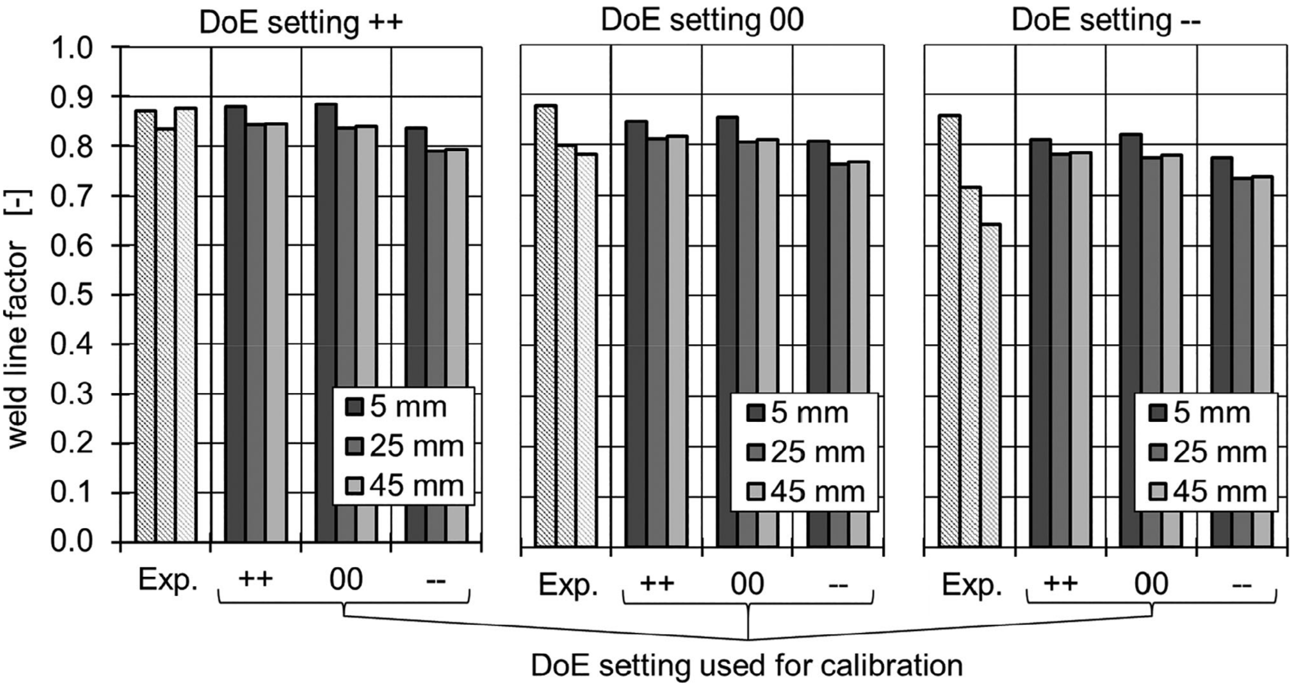

FIGURE 10 Weld line factors for polystyrene plates with rectangular flow barrier calculated using the reptation model

and the weld line factor predicted by the reptation model is achieved by calibration at the corresponding DoE setting. Calibration at the central DoE setting (00) also shows the best average results for all DoE settings with an error value of 0.0805. However, the differences between experimental data and prediction results are greater overall when using the reptation model than the interdiffusion model using the D_{DE} diffusion coefficient. The qualitative progression of the weld line factors over the distance to the flow obstacle is also worse than with the interdiffusion model. The reason for this is that the reptation model is much less sensitive to process conditions, which results in very similar predictions for all DoE settings. This results in bigger deviations to the experimental weld line strength due to its high dependency of the process.

4 | CONCLUSION

Different healing models for predicting the weld line strength of the amorphous thermoplastic polystyrene based on injection molding simulation were compared. The physical models considered were extended by experimental observations to improve the prediction accuracy. In particular, the increased weld line factors closer to the flow obstacle could be reproduced by considering the shear rate in the modeling.

A comparison of the calculation results of the individual models shows that the interdiffusion model using the interdiffusion coefficient D_{DE} according to Doi and Edwards provides the best representation of reality. In addition, when using this model, the best agreement of the qualitative difference between the weld line factors of the tensile bars at the different distances from the flow barrier can be achieved. The interdiffusion model with the interdiffusion coefficient D_B according to Bueche shows the largest deviations between prediction and reality. The quality of the results of the reptation model is set between the two models. However, although the reptation model generates the second-best results purely on the basis of deviations, the results show the same progression of weld line strength as a function of the distance from the flow obstacle in all calculations. So qualitatively the reptation model shows the worst prediction since it is less sensitive to process influences than the weld line strength in reality.

With the models described, the weld line strength can be predicted at an early stage of development after a single calibration at one process point, ideally the central point of all process settings used. Especially for frequently used materials, this results in big economic advantages. In addition, the models allow a better understanding of the relationship between different influencing factors on the weld line strength. However, the deviations of the prediction from reality also show that the presented model does not consider all influencing factors. Possible further influences to be investigated are the V-notch and the molecular orientation.

ACKNOWLEDGMENT

The research project (18132N) of the Forschungsvereinigung Kunststoffverarbeitung has been sponsored as part of the "industrielle Gemeinschaftsforschung und –entwicklung (IGF)" by the German Bundesministerium für Wirtschaft und Energie (BMWi) due to an enactment of the German Bundestag through the AiF. We would like to extend our thanks to all organizations mentioned.

We would also like to thank all members of the committee accompanying the project for their consulting on material selection, material testing, and model development. Open Access funding enabled and organized by ProjektDEAL.

ORCID

Jakob Onken https://orcid.org/0000-0002-5592-8637
Steffen Verwaayen https://orcid.org/0000-0002-3586-519X

REFERENCES

[1] S. Fellahi, A. Meddad, B. Fisa, B. D. Favis, *Adv. Polym. Technol.* **1995**, *14*(3), 169. https://doi.org/10.1002/adv.1995.060140302.

[2] I. Kühnert, *Grenzflächen beim Mehrkunststoffspritzgießen*, Schriftenreihe Kunststoffe, Bd. 1, Fördergemeinschaft für den Lehrstuhl Kunststofftechnik der TU Chemnitz e.V., FKTU, Chemnitz **2005**.

[3] L. Xie, *Materialwissenschaft und Werkstofftechnik 2, Polymerwerkstoffe und Kunststofftechnik, Bd*, 1st ed., Vol. 06, Papierflieger-Verl, Clausthal-Zellerfeld **2010**.

[4] T. Nguyen-Chung, *Strömungsanalyse der Bindenahtformation beim Spritzgießen von thermoplastischen Kunststoffen*, Technische Universität Chemnitz, Chemnitz **2001**.

[5] R. Seldén, *Polym. Eng. Sci.* **1997**, *37*(1), 205. https://doi.org/10.1002/pen.11663.

[6] S.-G. Kim, N. P. Suh, *Polym. Eng. Sci.* **1986**, *26*(17), 1200. https://doi.org/10.1002/pen.760261707.

[7] R. M. Criens, *Mater. Chem. Phys.* **1986**, *14*(1), 69. https://doi.org/10.1016/0254-0584(86)90019-2.

[8] S. C. Malguarnera, *Polym.-Plast. Technol. Eng.* **1982**, *18*(1), 1. https://doi.org/10.1080/03602558208067709.

[9] G. Mennig, *Mat.-wiss. Werkstofftech* **1988**, *19*(11), 383. https://doi.org/10.1002/mawe.19880191106.

[10] K. Tomari, S. Tonogai, T. Harada, H. Hamada, K. Lee, T. Morii, Z. Maekawa, *Polym. Eng. Sci.* **1990**, *30*(15), 931. https://doi.org/10.1002/pen.760301508.

[11] K. Yokomizo, Y. Banno, T. Yoshikawa, M. Kotaki, *Polym. Eng. Sci.* **2013**, *53*(11), 2336. https://doi.org/10.1002/pen.23487.

[12] D. J. Coyle, J. W. Blake, C. W. Macosko, *AIChE J.* **1987**, *33*(7), 1168. https://doi.org/10.1002/aic.690330711.

[13] K. Yokomizo, Y. Banno, M. Kotaki, *Polymer* **2012**, *53*(19), 4280. https://doi.org/10.1016/j.polymer.2012.07.042.

[14] G. Erhard, *Konstruieren mit Kunststoffen: [CD inside]*, 4th ed., Carl Hanser Verlag, München **2008**.

[15] T. Nguyen-Chung, G. Mennig, M. Boyanova, S. Fakirov, F. J. Baltá Calleja, *J. Appl. Polym. Sci.* **2004**, *92*(5), 3362. https://doi.org/10.1002/app.20335.

[16] T. Nguyen-Chung, *Rheol. Acta* **2004**, *43*(3), 240. https://doi.org/10.1007/s00397-003-0339-2.

[17] K. Cho, S. Ahn, J. Park, C. E. Park, J. H. An, *Polym. Eng. Sci.* **1997**, *37*(7), 1217. https://doi.org/10.1002/pen.11766.

[18] C.-C. Huang, Y.-Y. Wu, H.-T. Chang, Y.-J. Yang, *J. Polym. Eng.* **2012**, *32*(6-7), 365. https://doi.org/10.1515/polyeng-2012-0042.

[19] E. Debondue, J.-E. Fournier, M.-F. Lacrampe, P. Krawczak, *J. Appl. Polym. Sci.* **2004**, *93*(2), 644. https://doi.org/10.1002/app.20488.

[20] D. Grewell, A. Benatar, *Coupled Temperature, Diffusion and Squeeze Flowmodel for interfacial Healing Predictions*. Paper presented at: Proceedings of the Annual Conference of the Society of Plastics Engineers (ANTEC), Chaerlotte, USA. **2006**.

[21] M. Doi, S. F. Edwards, *The theory of polymer dynamics, The International series of monographs on physics*, Vol. 73, Clarendon Press, Oxford **1986**.

[22] H. H. Kausch, M. Tirrell, *Annu. Rev. Mater. Sci.* **1989**, *19*(1), 341. https://doi.org/10.1146/annurev.ms.19.080189.002013.

[23] J. G. Kovács, B. Sikló, *Polym. Test.* **2010**, *29*(7), 910. https://doi.org/10.1016/j.polymertesting.2010.06.003.

[24] Z. Shayfull, N. A. Shuiab, M. F. Ghazali, S. M. Nasir, Z. Nooraizedfiza, *Int. J. Eng. Technol.* **2011**, *11*(1), 111.

[25] T. C. Chang, E. Faison, *J. Injection Molding Technol.* **1999**, *3*(2), 61.

[26] E. Baur, S. Brinkmann, T. A. Osswald, N. Rudolph, E. Schmachtenberg, *Saechtling Kunststoff-Taschenbuch Ausg. 31*, 31st ed., Carl Hanser Verlag, München **2013**.

[27] I. S. Dairanieh, A. Haufe, H. J. Wolf, G. Mennig, *Polym. Eng. Sci.* **1996**, *36*(15), 2050. https://doi.org/10.1002/pen.10600.

[28] A. Y. Peng, D. C. Hsu, W.-H. Yang, R.-Y. Chang, *Prediction of the Weld-Line-Induced Strength Reduction for Injection-Molded Plastic Parts*. Paper presented at: Proceedings of the Annual Technical Conference of the Society of Plastics Engineers (ANTEC), Charlotte, USA. **2006**.

[29] J. Onken, C. Hopmann, *Z. Kunststofftech.* **2019**, *15*(2), 147. https://doi.org/10.3139/O999.02022019.

[30] J. Onken, C. Hopmann, *Kunststoffe* **2019**, *109*(12), 54.

[31] P. G. de Gennes, *J. Chem. Phys.* **1971**, *55*(2), 572. https://doi.org/10.1063/1.1675789.

[32] J. Onken, *Vorhersage der Bindenahtfestigkeit in ungefüllten amorphen Thermoplastbauteilen*, IKV - Berichte aus der Kunststoffverarbeitung, Institut für Kunststoffverarbeitung an der RWTH Aachen, Vol. 299, Mainz, Aachen **2020**.

[33] Y. H. Kim, R. P. Wool, *Macromolecules* **1983**, *16*(7), 1115.

[34] T. B. Juhl, J. de Claville Christiansen, E. A. Jensen, *J. Appl. Polym. Sci.* **2013**, *129*(5), 2679. https://doi.org/10.1002/APP.39000.

[35] A. Gooneie, S. Schuschnigg, C. Holzer, *Polymer* **2017**, *9*(12), 16. https://doi.org/10.3390/polym9010016.

[36] G. Agrawal, R. P. Wool, W. D. Dozier, G. P. Felcher, J. Zhou, S. Pispas, J. W. Mays, T. P. Russell, *J. Polym. Sci., Part B: Polym. Phys.* **1996**, *34*(17), 2919. https://doi.org/10.1002/(SICI)1099-0488(199612)34:17<2919:AID-POLB6>3.0.CO;2-L.

[37] T. J. Coogan, D. Kazmer, *Rapid Prototyping J.* **2017**, *23*(3), 551. https://doi.org/10.1108/RPJ-03-2016-0051.

[38] K. A. Welp, R. P. Wool, S. K. Satija, S. Pispas, J. Mays, *Macromolecules* **1998**, *31*(15), 4915. https://doi.org/10.1021/ma971692n.

[39] T. A. Osswald, N. Rudolph, *Polymer rheology: Fundamentals and applications*, Hanser Publications, Cincinnati, OH **2015**.

[40] M. L. Williams, R. F. Landel, J. D. Ferry, *J. Am. Chem. Soc.* **1955**, *77*(14), 3701. https://doi.org/10.1021/ja01619a008.

[41] G. Menges, F. Wortberg, W. Michaeli, *Kunststoffe* **1978**, *68*(1), 47.

[42] G. Menges, E. Haberstroh, W. Michaeli, E. Schmachtenberg, *Menges Werkstoffkunde Kunststoffe*, 6th ed., Carl Hanser Verlag, München **2011**.

[43] T. A. Osswald, J. P. Hernández-Ortiz, *Polymer processing: Modeling and simulation*, Carl Hanser Verlag, München **2006**.

[44] J. E. Mark, *Physical properties of polymers handbook*, Springer Science+Business Media, LLC, New York, NY **2007**.

[45] L. J. Bastien, J. W. Gillespie, *Polym. Eng. Sci.* **1991**, *31*(24), 1720. https://doi.org/10.1002/pen.760312406.

[46] F. S. Bates, *Science (New York, N.Y.)* **1991**, *251*(4996), 898. https://doi.org/10.1126/science.251.4996.898.

[47] K. Jud, H. H. Kausch, Fracture mechanical studies of the strength resulting from polymer interdiffusion, Paper presented at: International Conference on Fracture (ICF5), Cannes, Frankreich. **1981**.

[48] F. Bueche, *J. Am. Chem. Soc.* **1952**, *20*(12), 1959. https://doi.org/10.1063/1.1700349.

[49] M. Stommel, M. Stojek, W. Korte, *FEM zur Berechnung von Kunststoff- und Elastomerbauteilen*, 2nd ed., Carl Hanser Verlag, München **2018**.

[50] C. Hopmann, J. Onken, *Adv. Polym. Technol.* **2018**, *26*, 1. https://doi.org/10.1002/adv.21933.

How to cite this article: Onken J, Verwaayen S, Hopmann C. Evaluation of healing models to predict the weld line strength of the amorphous thermoplastic polystyrene by injection molding simulation. *Polym Eng Sci*. 2020;1–13. https://doi.org/10.1002/pen.25614